

Structure-Processing-Property Correlations in Solution Processed, Small Molecule, Organic Solar Cells

Benjamin H. Wunsch, Mariacristina Rumi, Naga Rajesh Tummala, Chad Risko, Dun-Yen Kang, Xerxes Steirer, Jeremy Gantz, Marcel M. Said, Neal R. Armstrong, Jean-Luc Brédas, David Bucknall, and Seth R. Marder

Supporting Information

Experimental

Organic solar cell device fabrication and testing: Active layer inks were prepared at 15 mg/mL, typically 10 – 20 mL. Anhydrous chloroform and chlorobenzene (Sigma Aldrich) were degassed for 30 min by bubbling N₂ through the solvent. PCBM (Nano-C) was used as received. BD and BD6 were synthesized as described previously.¹ The organic semiconductors were weighed out, in air, into individual glass vials with Teflon lined screw caps and then transferred to a N₂ glove box where the solvent was added. Stock solutions of each semiconductor were prepared first and allowed to stir while heating at 60 °C for chlorobenzene and 40 °C for chloroform for 1 hr. Blends of donor and PCBM were prepared by adding the appropriate volume of each stock to a new vial (typically 10 mL total volume) and stirring at 60 °C for 1 hr.

ITO substrates (Colorado Concepts, 1" × 1") are prepared by sequentially scrubbing with a 10 v/v% aqueous Triton-X solution using a Softec cleaning cloth then sonicating for 15 min in Triton-X solution using a Branson 2510 sonicator. This process is repeated with filtered water (Nanopore) and then 200 proof ethanol (Decon Labs). The ITO is jet dried with N₂ and then oxygen plasma activated in a Harrick Plasma, PDC-32G at 400 mTorr for 10 min. Immediately after, the sample is coated with Clevios P VP AL4083 PEDOT:PSS solution by spin coating for (1) 10 s, 1000 RPM, 1512 RPM s⁻¹, (2) 60 s, 5000 RPM, 5500 RPM s⁻¹. The PEDOT:PSS is applied and spun twice. The PEDOT:PSS coated sample is placed on a hot plate at 140 °C in ambient atmosphere and allowed to sit 10 min. Immediately after, while the substrate is still hot, it is transferred into a N₂ glove box.

Active layers are prepared by spin coating the blended donor:PCBM solutions onto the PEDOT:PSS/ITO substrates. In most cases, to increase through-put, a single ITO substrate is scribed into ~0.5" × 0.5" quarters and each quarter coated with a different blend and/or set of processing conditions. The quartered substrate is then pieced together and the top-electrodes deposited (*vide infra*). Substrates are spun within 30 min of their annealing at 140 °C. Each blended solution is filtered through a 0.45 μm PTFE Whatman filter using a 1 mL PDMS syringe, directly onto the substrate, which is immediately spun at the appropriate conditions. For

all spin casting, the spin time is 60 s and the acceleration is 1500 RPM s⁻¹; the spin speed is either 1000 or 2000 RPM, depending on the parameter set. Substrates were then transferred via a carrier bomb to a second glove box where the substrate was loaded into the thermal deposition chamber for top-electrode fabrication.

A metal mask consisting of a 5 × 5 checkerboard array of 0.019 cm² holes is used to pattern the top-electrode (cathode); the area of the hole defines an individual cell in the device. 8 nm of LiF is deposited at 0.1 Ås⁻¹, followed by 100 nm of aluminum deposited at 1 Ås⁻¹. Deposition is at 10⁻⁷ torr. The finished devices are measured within 1 hr of electrode deposition, with some samples checked within 24 – 48 hour for consistency of output. For samples that are annealed, the device is set on a hot plate pre-warmed to the target temperature, in the glove box, and allowed to anneal for 5 min, after which the sample is set on a metal surface to cool and subsequently measured. OPV measurements were made on a custom build stage in a N₂ glove box using a 1.5 AM filtered white light. The base ITO is contacted by a metal clip, and each cell is accessed independently using a gold wire. Typical voltage sweeps are -1 to 1.5 V. Statistical analysis of the device properties was carried out using ANOVA methods in OriginPro™ 8.5 software.

AFM measurements: Analysis is carried out on an Agilent Technologies 5600LS Scanning Probe Microscope in AC mode (dynamic vertical mode or intermittent contact mode) using tips from Asylum Research, model “AC240TS”, with nominal frequency and force constant of 70 kHz and 2 N/m, respectively, or from Mikromash, Model “Ultrasharp NSC35/no Al”, with 315 kHz nominal frequency and 14 N/m force constant. The cantilevers are operated at -0.1 kHz from their resonance frequency. Scan speeds are in the range 0.3 -1.0 lines/s with a sampling rate of 512 pixels per line in the fast scanning direction (perpendicular to the cantilever body; horizontal axis in the images included in this paper). Topography images are processed within the Gwyddion software package² by scaling the height values to the median for each line and the subtracting a planar background. The color scale for height parameter is generally adjusted to exclude the values in the tails of the distribution (to improve contrast between features), but without affecting the linearity.

Samples are prepared as follows: Solutions of BD6, BD, and PCBM in chloroform and chlorobenzene (30.0 mg/mL in all cases) are prepared. The chlorobenzene solutions are set to stir on a hot plate for one hour at 60 °C and then one hour at 40 °C. The chloroform solutions are stirred for one hour at 40 °C. After allowing the solutions to cool to room temperature, aliquots are mixed and diluted to obtain the desired compositions for a total solids concentration of 15 mg/mL. Glass substrates (1” × 1”) are sonicated in 5% v/v Triton X/water for 15 min, in distilled water for 15 min, and then in ethanol for 15. The substrates are dried under a flow of nitrogen gas and cleaned by oxygen plasma for 5 min. PEDOT:PSS (Clevios P VP AI4083, filtered with a 0.45 µm glass fiber Whatman filter) is deposited on the ITO slides shortly after plasma cleaning, using the following spin coating conditions: step 1) 10 s, 1000 RPM, 1540 RPM s⁻¹, step 2) 60 s, 5000 RPM, 5500 RPM s⁻¹ and repeating steps 1-2 a second time after dispensing a fresh amount of solution. Films from the mixed solutions described above and from the donor-only solution (after dilution to 15 mg/mL) are deposited on PEDOT:PSS by spin coating at 1000 or 2000 RPM, with acceleration = 1540 RPM s⁻¹ and time = 60 s. After these

films had been characterized, they are annealed at 100 °C for 5 min (\pm 10 s) on a hot plate under nitrogen. At the end of the annealing time, the samples are removed from the hot plate and placed on a metal plate for rapid cooling. The characterization measurements are repeated after the annealing step. The same samples are used for measurement of the transmission spectra and fluorescence emission spectra.

Depth profiling by D-SIMS: Depth profiling of thin films was performed by dynamic secondary ion mass spectrometry on a TOF SIMS 5.3 system (by IONTOF GMBH), at the Georgia Tech Institute for Electronics and Nanotechnology. The primary ion was Bi^+ , rastered over a $150 \mu\text{m} \times 150 \mu\text{m}$ area. A Cs gun was used for the sputtering over a $320 \mu\text{m} \times 320 \mu\text{m}$ area (with the same center as the raster area). Secondary ions (with negative polarity) were collected in the non-interlaced acquisition mode, with 1.0 s sputter time and 0.5 s pause time for each scan (data collection lasted about 3.5 s for 128×128 resolution of the raster area after each sputtering interval). An electron flood gun was turned on during sputtering, to reduce charging effects. The base pressure in the sample chamber during measurements was below 5×10^{-8} mbar. Under the chosen experimental conditions, the signal intensities for ions C^- and S^- , are very close to the saturation value and thus are affected by a large uncertainty (even after Poisson correction). We have thus chosen to use ion CH^- as the reference fragment for the organic layer, instead of C^- . Two fragments that can be associated with the donor component of the film are SN^- (45.973 u) and C_4S^- (79.974 u). The onset of the PEDOT:PSS layer during sputtering can be identified by the increase over the noise level of the signals at 23 u (assigned to Na^-)¹ and at 46 u (assigned to CH_2O_2^-).

It should be mentioned that the D-SIMS data are reported as a function of sputter time, which is related to the thickness of the ablated layer and thus the depth in the film. The film depth increases with, but it is not proportional to, the sputter time. We have found on control samples that the ablation rate is significantly slower at low sputter times than later in the measurement. Also, the ablation rate was strongly dependent on the composition of the film, being slower at higher content of PCBM (and thus would not be constant in samples with a composition gradient). For the case in Figure 4, the sharp increase in the signals starting at 420 s for the chlorobenzene film and 780 s for the chloroform film corresponds to the interface with the PEDOT:PSS layer. The PEDOT:PSS layer is reached after longer sputter time in the chloroform film because this is thicker than the chlorobenzene one.

Sample for depth profiling measurements were prepared as follows. Solutions of BD6, BD, and PCBM in chlorobenzene or chloroform (15.0 mg/mL in all cases) were prepared. The solutions were set to stir at room temperature for at least one hour. Aliquots were mixed to obtain mixed solutions of desired composition and the mixed solutions were stirred for one hour. Silicon wafers with a 300 nm layer of thermal oxide (from University Wafers, type #1203) were cut into squares ($1'' \times 1''$) and sonicated in 5% v/v triton X/water for 20 min, in distilled water for 20 min, and then in ethanol for 20 min. The substrates were then dried under a flow of nitrogen gas

¹ In many formulations, including the one used in our lab, polystyrene sulfonate is present in PEDOT:PSS as a sodium salt.

and cleaned by oxygen plasma for 3 min. PEDOT:PSS (Clevios P VP AI4083, filtered with a 1.0 μm GF/B w/GMF Whatman filter) was deposited on the substrates, using the following spin coating conditions: step 1) 10 s, 1000 rpm, 1540 rpm/s, step 2) 60 s, 5000 rpm, 5500 rpm/s and repeating steps 1-2 a second time after dispensing a fresh amount of suspension. The PEDOT:PSS coated substrates were then baked at 140 $^{\circ}\text{C}$ for 10 min. Films from the mixed solutions and the donor-only solutions were deposited on the PEDOT:PSS layer by spin coating with acceleration = 1540 rpm/s and time = 60 s at 1000 or 2000 rpm. After film preparation, each sample was cut in rectangular halves. One of the sections was annealed at 100 $^{\circ}\text{C}$ for 5 min (± 10 s). The as-prepared and annealed sample pieces were then used for D-SIMS measurements under the same conditions.

Fluorescence measurements: Fluorescence emission spectra were recorded on a Horiba Jobin Yvon Fluorolog III spectrometer with a cooled R928 photomultiplier tube as a detector. The films were mounted on a solid sample holder, with the film side facing the incident beam. The excitation wavelength was 500 nm. The angle of incidence to the film surface was approximately 0° with respect to the normal to the film surface. The collection was performed in the “front face” configuration (ca. 20° between the excitation beam and line of detection). Background signal due to the substrate was subtracted and the spectra corrected to account for the wavelength dispersion of the instrument response.

Ellipsometry measurement: Ellipsometry measurements were carried out on a M2000 ellipsometer (Woollam) at the Georgia Tech Institute for Electronics and Nanotechnology. The measurements were performed over five incident angles (60° to 80° in 5° steps) and in the wavelength range 370 – 1690 nm. The data were processed using the CompleteEASE software (Woollam) by building a model for the optical layers in the samples. The thickness and the complex refractive index of the top layer were obtained by determining the best fit of the experimental data to the model. Optical parameters and thicknesses for the underlying layers were determined using a similar procedure applied to measurements on control samples (Si/SiO₂ substrate only; Si/SiO₂ substrate with PEDOT:PSS layer) and then kept fixed in samples with additional layers. In the case of the Si/SiO₂ sample, only the thickness of the silica layer and that of a thin (ca. 1.5 nm) interface layer under the silica one were free parameters of the fitting, whereas literature values for the Si and SiO₂ optical constants were used. A B-spline model with Kramer-Kronig constraints was used to describe the complex refractive index ($\tilde{n} = n + ik$) for each of the organic layers (PEDOT:PSS and donor:PCBM mixture). The uncertainty in the thickness is estimated to be about ± 2 nm, based on changes in fitting results when the model is changed or certain parameter constraints are relaxed without significant changes in the goodness of the fit. The error on the organic layer thickness from a single fitting attempt was always better than 0.3 nm.

Molecular dynamics simulations: The OPLS-AA force-field parameters^{3, 4} were used with Gromacs 4.5.4^{5, 6} for the MD simulations within the NPT (constant number of particles, constant pressure and temperature) ensemble. Random initial configurations of 400 BD and BD6

molecules were generated within a cubic box. These initial configurations were run for 1 ns each at 900 K and 800 K, equilibrated for 5 ns at 500 K (at 700 K for BD6, BD8, and BD9), and then further cooled to 150 K and run until the volume became constant. The final configurations were used to evaluate the melt transitions via a series of 600 ps runs at 25 K intervals through the temperature range 150 – 600 K.⁷ The resulting volume vs. temperature curves were split into 3 parts, fit with straight lines ($R^2 > 0.99$), and the intersection of lines used to compute the melting temperatures. As expected, there is a gradual increase in the melting temperature as the alkyl side-chain length increases (Figure S17).

To evaluate the blend miscibility, 9 mole fractions, ranging from 0.1 through 0.9, of BDX/PCBM mixtures for BD and BD6 molecules were simulated. For each mole fraction, a total of 400 molecules were randomly placed in a simulation box and equilibrated for 1 ns at 900 K, and 1 ns at 800 K, further cooled to 700 K for 2.5 ns, with a final simulation at 300 K for 2.5 ns. The simulations were repeated three times at 700 K and 300 K, and the resulting thermodynamic quantities were used to compute the error in the Flory-Huggins parameter and verify the validity of the equilibration procedure. In addition, the cohesive energy density and corresponding Hildebrand⁸ and Hansen⁹ solubility parameters were determined following procedures described elsewhere.^{10, 11}

Grazing-Incidence X-ray Scattering: Samples for GIWAXS and GISAXS measurements are prepared as described for the organic solar cell fabrication (see above) with the following modifications: $2.5 \times 2.5 \text{ cm}^2$ SiO_2/Si substrates were used instead of ITO. A solution of 6:1 v:v deionized water:PEDOT:PSS (as received) is spin-cast at 60 s, 4000 RPM, 5000 RPM s^{-1} on the cleaned substrates followed by thermal annealing at $140 \text{ }^\circ\text{C}$ for 10 min. Semiconductor blend solutions are prepared and spin-cast as done for the solar cell fabrication, using the same processing conditions (but no LiF or electrode was deposited).

GIWAXS and GISAXS measurements were performed at Beamline I07 – Surface and Interface Diffraction at the Diamond Light Source, Harwell Science and Innovation Campus, Oxfordshire, UK, and at the SWING Beamline at the Soleil Synchrotron, L'Orme des Merisiers Saint-Aubin, France. For GIWAXS: On I07, photon wavelength was $\lambda = 1.378 \text{ \AA}$, sample-to-detector distance = 33 cm, using a Pilatus 2M CCD Detector with a pixel size of $172 \times 172 \text{ }\mu\text{m}^2$, on SWING, $\lambda = 1.033 \text{ \AA}$, sample-to-detector distance = 59 cm, using a Princeton 2D CCD Detector with a pixel size of $168 \times 168 \text{ }\mu\text{m}^2$. For GISAXS, on I07, $\lambda = 1.378 \text{ \AA}$, sample-to-detector distance = 295 cm, using a Pilatus 2M CCD Detector with a pixel size of $172 \times 172 \text{ }\mu\text{m}^2$. The incident angle range was $\alpha_i = 0.10^\circ - 0.20^\circ$. Silver behenate was used as a calibration standard. Images were analyzed using FIT2D software to extract 1D integrated profiles.¹²

The *in situ* GIWAXS measurements were performed at beamline 8-ID-E at Argonne National Laboratory. The monochromated energy of the X-ray source was 7.35 keV (X-ray wavelength = 1.687 \AA) and the incidence angle was 0.20° . The GIWAXS instrument at the end station was equipped with a Pilatus 2M CCD detector. The sample-to-detector distance was 204 mm. The samples were placed in a vacuum chamber with a pressure of about 10^{-3} torr through the whole

experiments. This image processing was performed with MATLAB[®]-based software, GIXSGUI, developed by Zhang Jiang in Sector 8 at Argonne National Laboratory.

Differential Scanning Calorimetry: Solutions of each semiconductor (PCBM, BD, BD6) are prepared separately in chloroform (Sigma Aldrich) in glass vials with Teflon lined caps; 15 mg mL⁻¹, 5-10 mL. Solutions are stirred at 60 °C for 1 hr. Blended solutions are prepared by mixing appropriate volume of each semiconductor stock solution (500-600 μL total volume) and stirring at 60 °C for 1 hr. For chlorobenzene samples, each blended chloroform solution had solvent removed on a rotary evaporator, leaving only a solid film in the vial. Chlorobenzene is added (500-600 μL total volume) and stirred at 60 °C for 1 hr.

For each sample, a microscope glass slide is sonicated 30 min in acetone, 30 min in absolute ethanol, and then N₂ jet dried. Glass slides are loaded into a N₂ box with the blended solutions. Glass slides are set on top of a plastic vial cap to prevent wicking of solvent over the slide edge. Blended solutions are deposited on top of each glass slide and allowed to dry (~24 hr). The films are removed from the glove box and each film individually scraped into a powder using a razor blade. The powder is collected into a pre-weighed TA Instruments Tzero[™] aluminum pan. The pan is sealed with a pre-weighed hermetic lid and the sample then weighed; typical sample masses are 3-6 mg per sample. The sealed sample pans are cleaned gently with a cotton swap and chloroform prior to weighing, to remove traces of organic powder. Analysis is carried out on a TA Instruments Q200[™] Differential Scanning Calorimeter. Samples are run under 50 mL min⁻¹ N₂ flow from -60 to 200 °C for three heating/cooling cycles at a heating rate of $\beta = 10 \text{ °C min}^{-1}$, and the resulting thermograms analyzed using TA Instruments Universal Analysis[™] software.

Supplemental Figures and Tables

Table S1. Test of statistical significance of difference in device property means at 95% confidence level for BD:PCBM and BD6:PCBM solar cells.

	Device Sets	Variable Tested ^{a,b}		
		V_{oc}	J_{sc}	% PCE
Reproducibility Comparison	BD high	T	T	F
	BD low	T	F	T
	BD6, CB	F	F	F
	BD6, CF	F	T	F
Performance State Comparison	BD6, CB vs. CF	F	T	F
	BD high / BD6	T	T	T
	BD low / BD6	T	T	T
	BD high / BD low	T	T	T

a: Variables tested using one-way ANOVA.

b: T = null hypothesis true; means are not significantly different at 95% confidence. F = null hypothesis false; means are significantly different at 95% confidence.

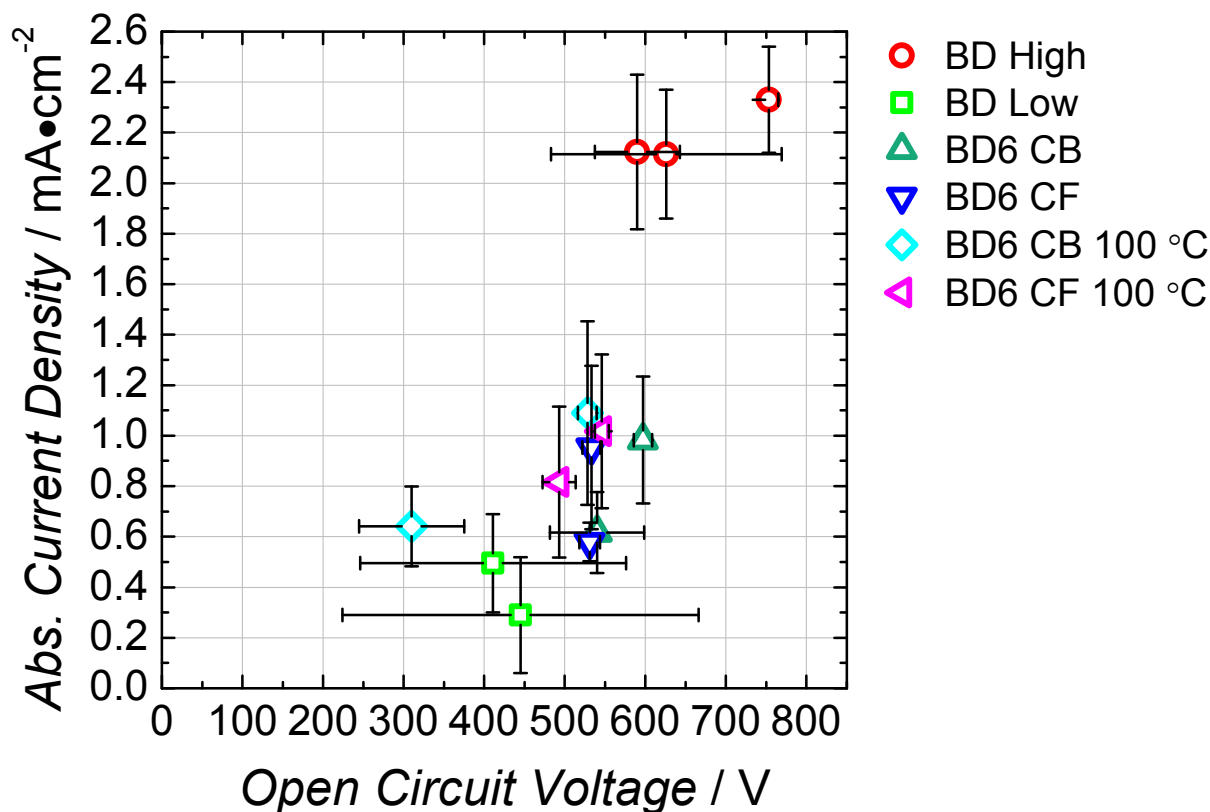


Figure S1. Scatter plot of reproduction devices for the BD:PCBM and BD6:PCBM systems, showing the absolute short current density (J_{sc}) as a function of open circuit voltage (V_{oc}). Symbols demarcate the average value for all cells (up to 25) in a reproduction device; error bars represent one standard deviation from the mean. For the BD6 system, two processing formulations were used as representatives of the BD6 device clustering. The performance states are those BD6:PCBM devices annealed at 100 °C for 5 min. The as-prepared BD6:PCBM devices are included for completeness, and to show the marginal effect of the post-processing annealing compared to the fluctuation in data.

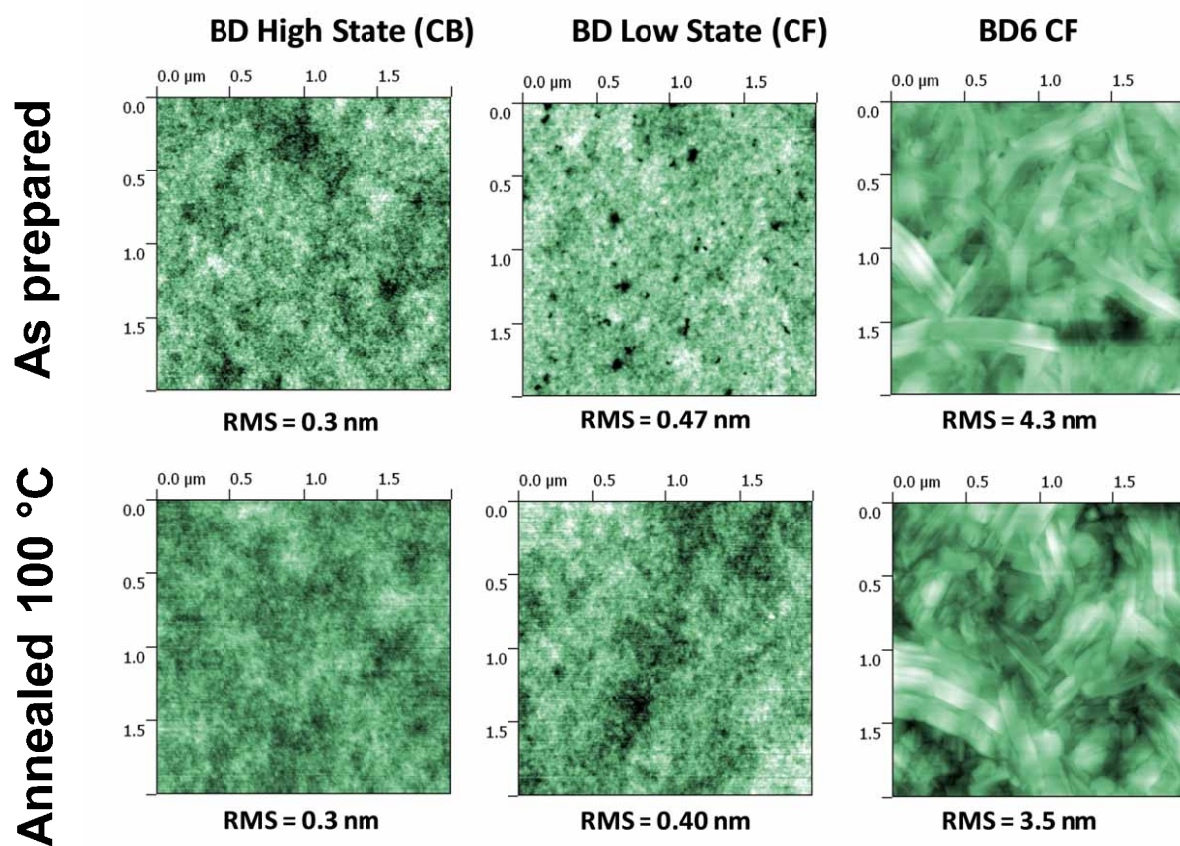


Figure S2. Atomic force microscopy topography scans of performance state thin films for BD:PCBM and BD6:PCBM as-prepared and after annealing at 100 °C for 5 min, demonstrating that the surface textures do not change significantly with the annealing process.

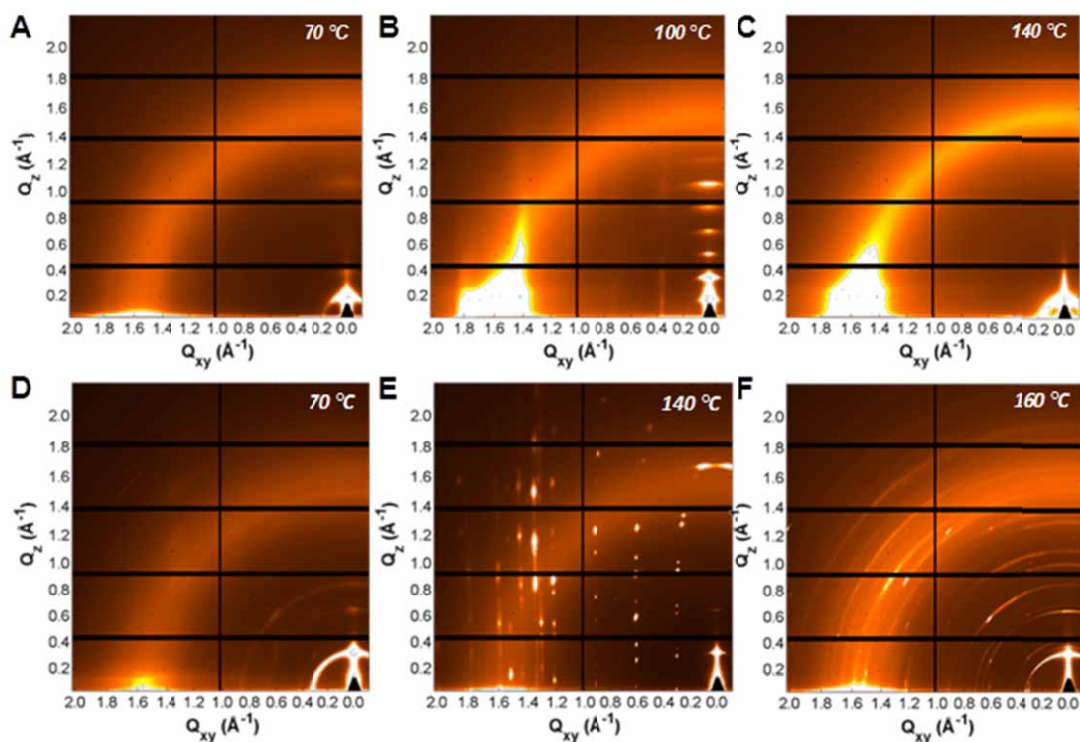


Figure S3. 2D-GIWAXS patterns measured for thin films of (A-C) BD and (D-F) BD6 as a function of annealing temperature. BD annealed at (A) 70 °C, (B) 100 °C and (C) 140 °C. (D) BD6 annealed at (D) 70 °C, (B) 140 °C and (C) 160 °C. All annealing performed for 10 min. Scattering patterns taken at room temperature (post-anneal). Annealing BD at 70 °C leads to no change in the 2D GIWAXS pattern, whereas at 100 °C, a series of out-of-plane reflections appears with $d_z = 32.3$ Å. These (00k) reflections have a different d -spacing from the weak intensity peak observed in the as-prepared film and represent a new ordering in the BD system. The magnitude of the d -spacing and the orientation of the reflections suggest the BD molecules are forming lamellar stacks through the thickness of the thin film; however, the orientation of the π -system with respect to the film substrate cannot be determined. There is also evidence of weak in-plane ordering of the lamellae, with a $d_{xy} = 16.8$ Å. Annealing further, to 140 °C, causes the diffraction intensity to disappear, indicating the film has become mostly amorphous.

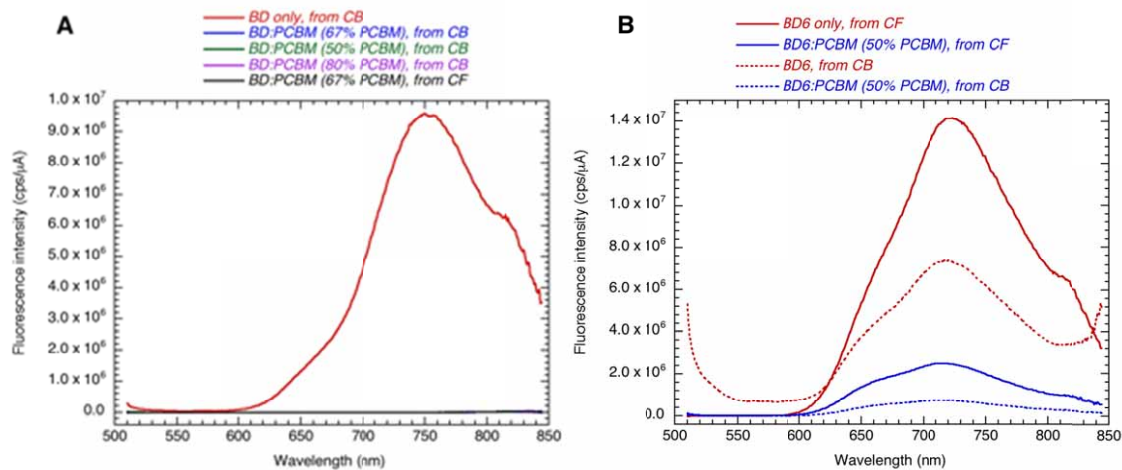


Figure S4. Fluorescence spectra of thin films of (A) BD and (B) BD6 for varying wt% of PCBM and casting solvent (CB = chlorobenzene, CF = chloroform).

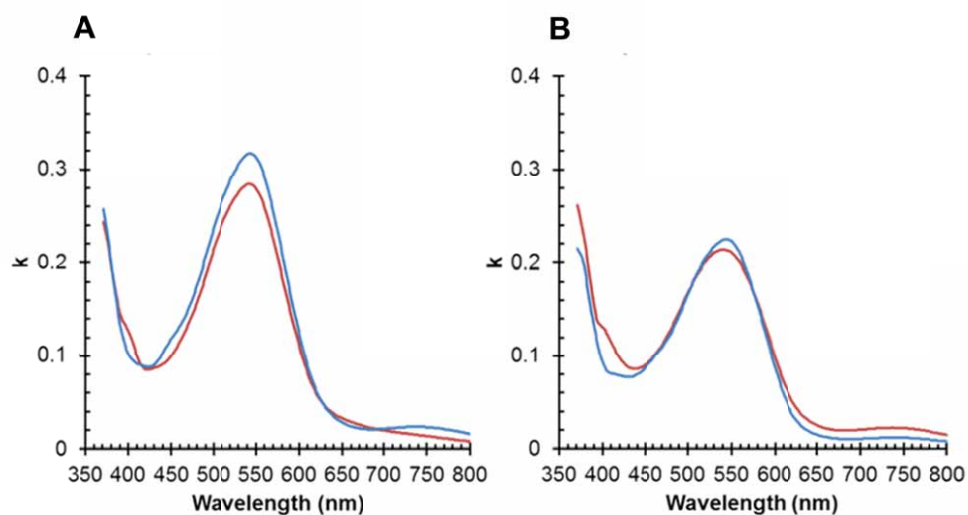


Figure S5. Absorption coefficient k (imaginary component of refractive index) obtained from spectroscopic ellipsometry for films of (A) a 1:1 BD:PCBM blend, (B) a 1:1 BD6:PCBM blend. Red lines: films cast from chlorobenzene solutions, blue lines: films cast from chloroform solutions.

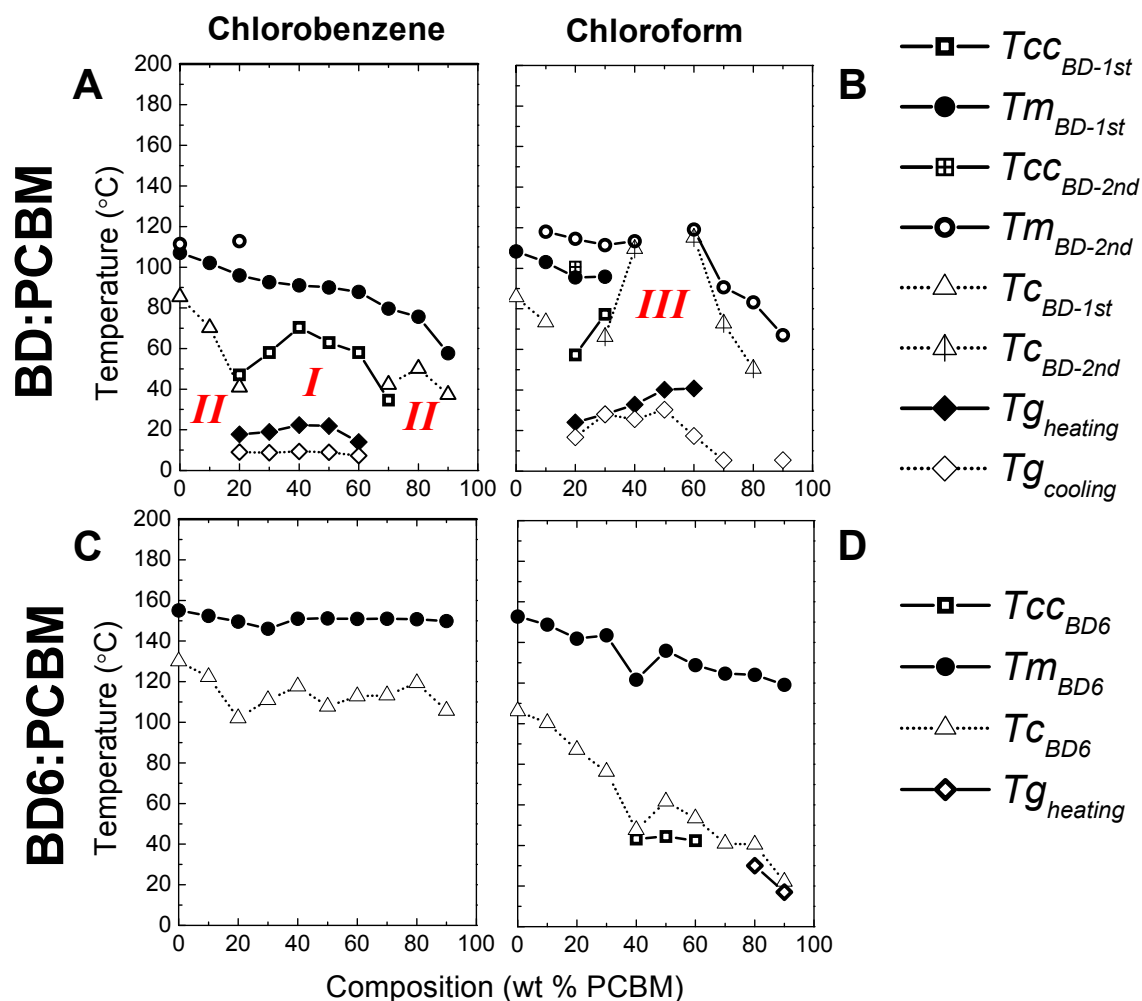


Figure S6. Phase diagrams of the second heating/cooling cycle derived from DSC for the BD:PCBM and BD6:PCBM systems for the deposition solvents chlorobenzene and chloroform. Cycles are taken from -60 – 200 °C. The phase diagram has been truncated from the full -60 – 200 °C to focus only on the temperature range in which transitions are observed. The roman numerals refer to regions described in the text. T_{cc} – cold crystallization temperature, T_m – melting temperature, T_c – recrystallization temperature, T_g – glass transition temperature. The 1st and 2nd refer to sequential exo- or endothermic transitions occurring at increasing temperature within the same cycle.

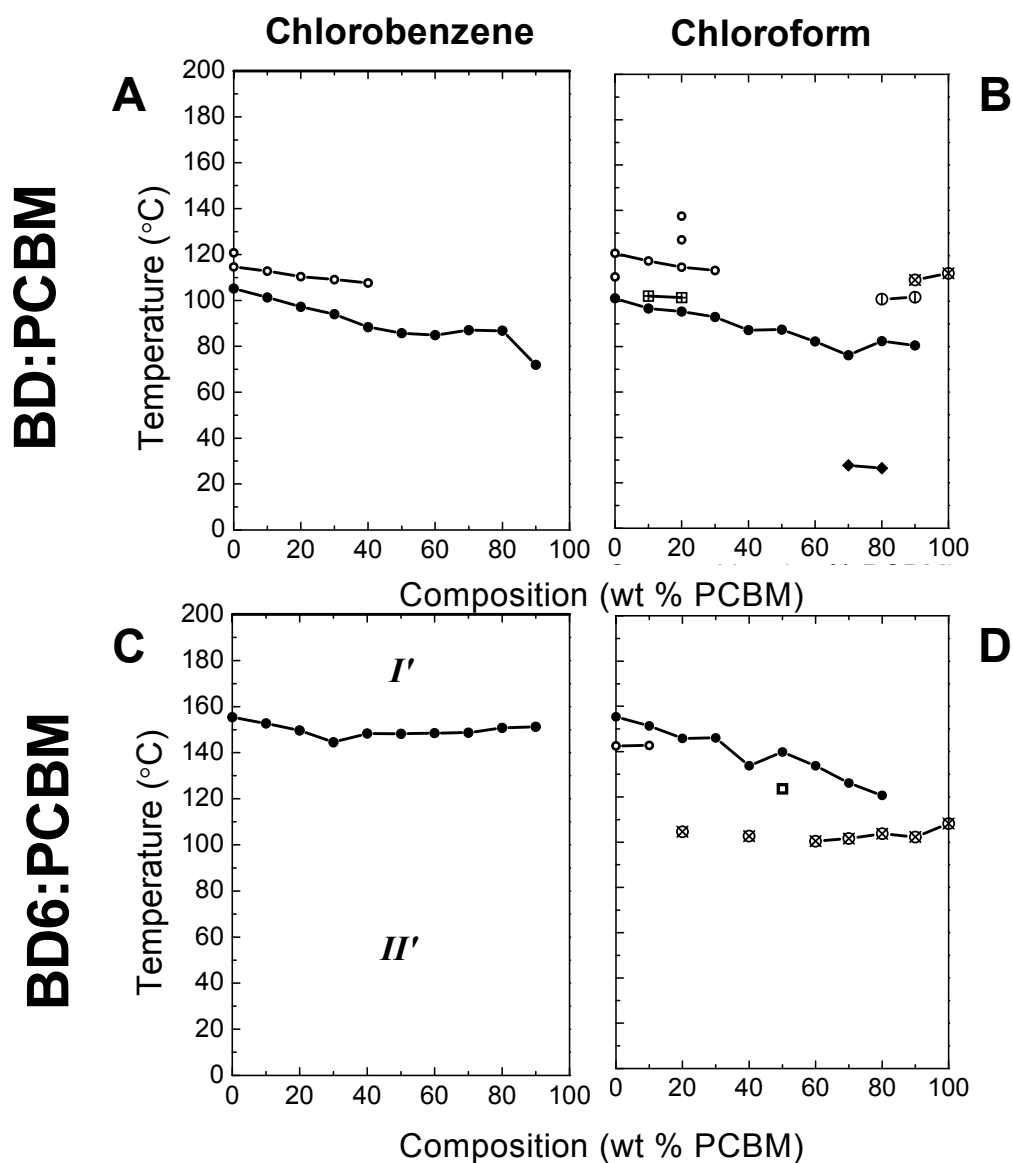


Figure S7. Phase diagrams of the 1st heating cycles derived from DSC for the BD:PCBM and BD6:PCBM systems for the deposition solvents chlorobenzene and chloroform. Cycles are taken from -60 – 200 °C. The phase diagram has been truncated from the full -60 – 200 °C to focus only on the temperature range in which transitions are observed. **Legend:** (A & B) Filled circle: 1st BD endothermic transition. Open circle: 2nd / 3rd BD endothermic transitions (melting point). Line circle & crossed circle: high PCBM endothermic transitions. Crossed square: BD cold crystallization. Filled square: cold crystallization of PCBM. Filled diamond: glass transition. (C & D) Open circle: 1st BD6 endothermic transition. Filled circle: 2nd BD6 endothermic transitions. Crossed Circle: high PCBM endothermic transition. Open square: cold crystallization of BD6.

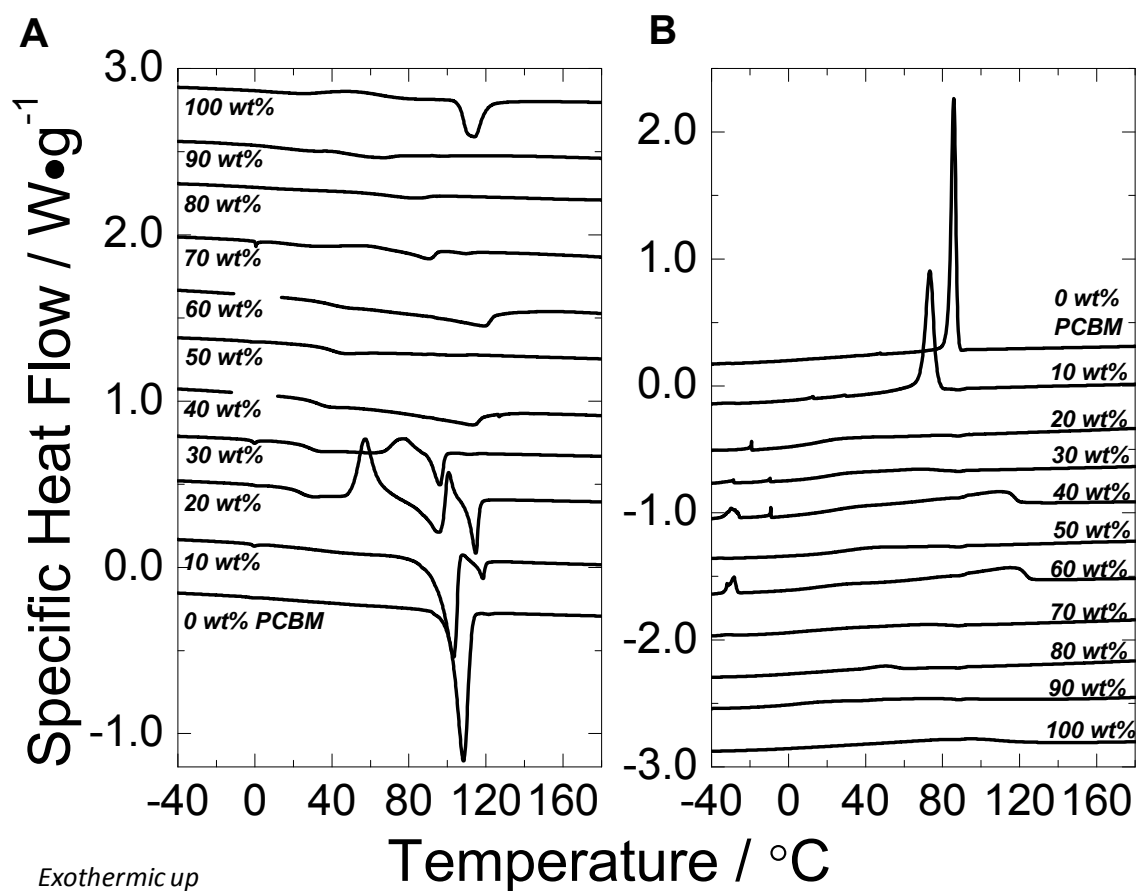


Figure S8. Differential scanning calorimetry thermograms of BD:PCBM composition series mixtures dried from chloroform for (A) 2nd heating cycle and (B) 2nd cooling cycle. Cycles are taken from -60 $^{\circ}C$ to 200 $^{\circ}C$. Thermograms have been truncated to show the thermal transitions better. Thermograms have been offset for better display. Each composition is demarcated by weight percent PCBM.

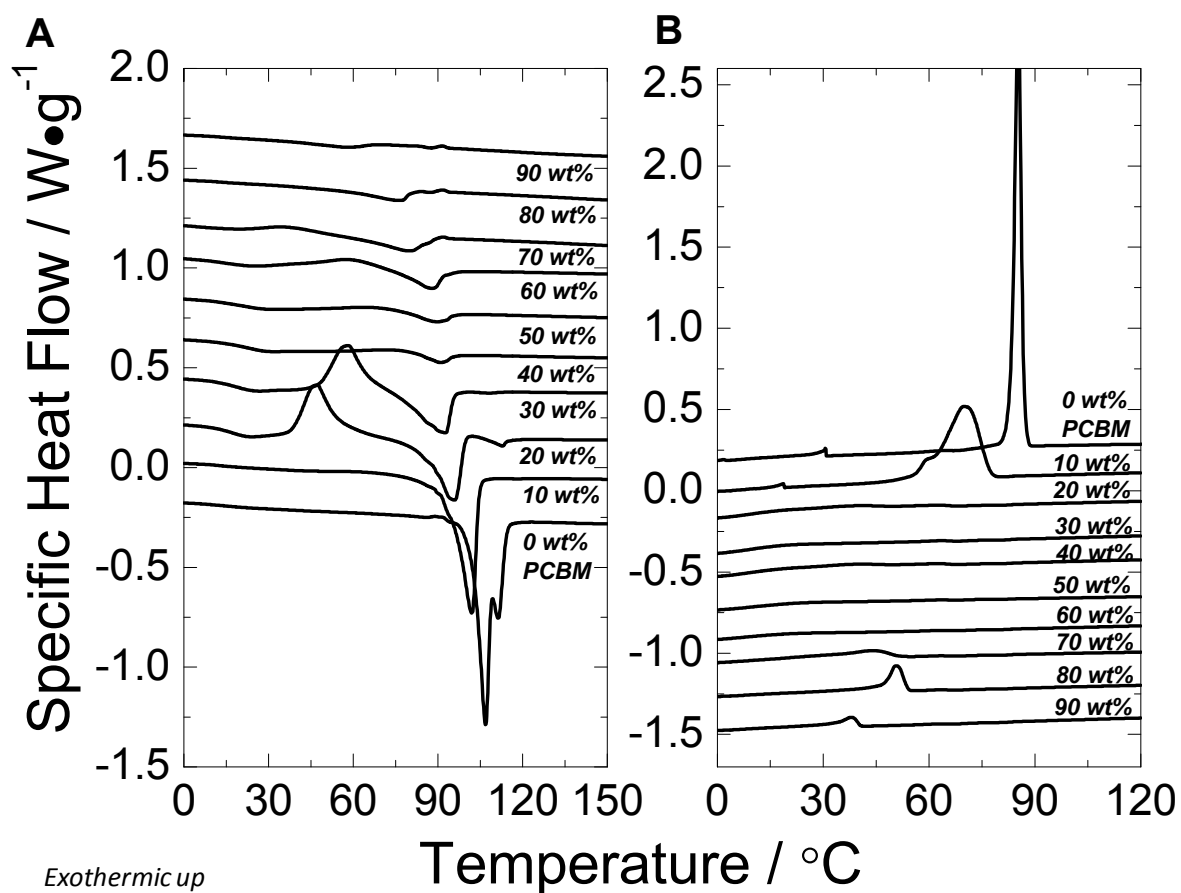


Figure S9. Differential scanning calorimetry thermograms of BD:PCBM composition series mixtures dried from chlorobenzene for (A) 2nd heating cycle and (B) 2nd cooling cycle. Cycles are taken from -60 $^{\circ}\text{C}$ to 200 $^{\circ}\text{C}$. Thermograms have been truncated to show the thermal transitions better. Thermograms have been offset for better display. Each composition is demarcated by weight percent PCBM.

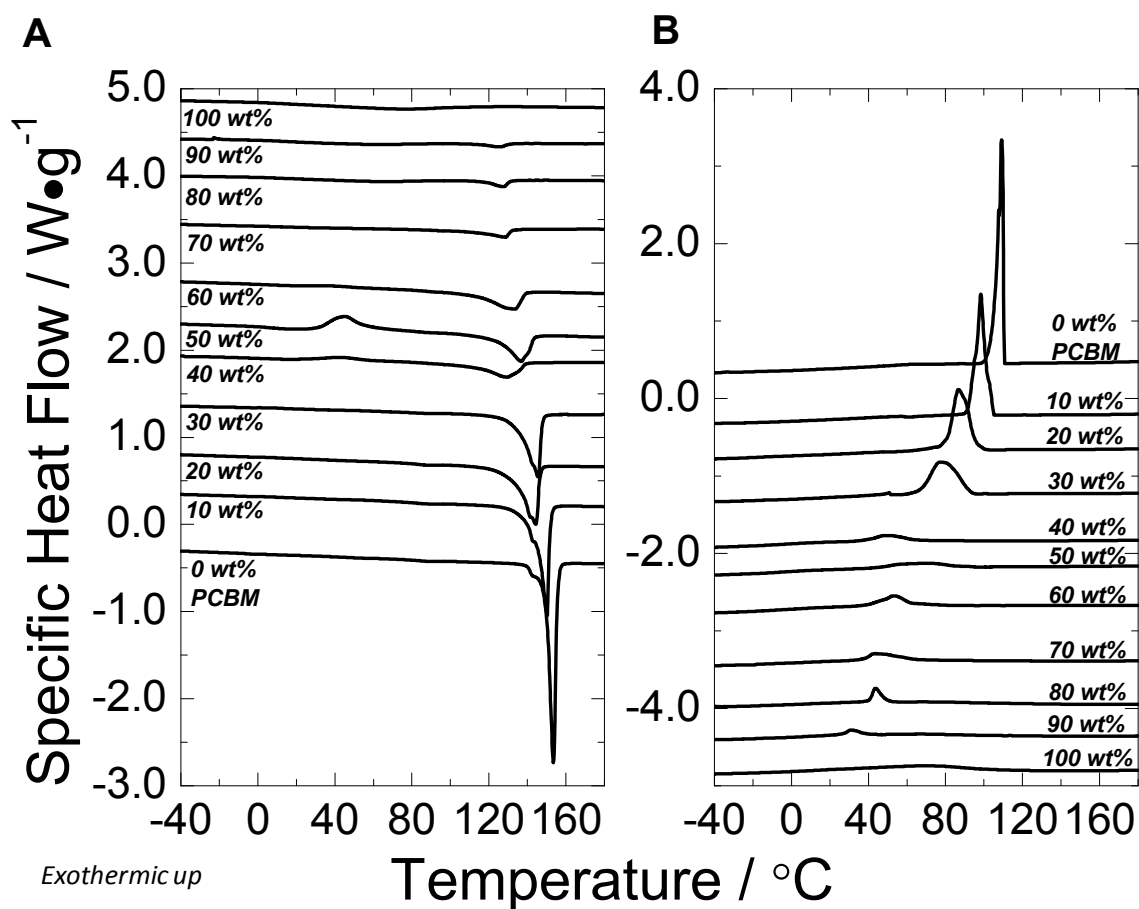


Figure S10. Differential scanning calorimetry thermograms of BD6:PCBM composition series mixtures dried from chloroform for (A) 2nd heating cycle and (B) 2nd cooling cycle. Cycles are taken from -60 $^{\circ}\text{C}$ to 200 $^{\circ}\text{C}$. Thermograms have been truncated to show the thermal transitions better. Thermograms have been offset for better display. Each composition is demarcated by weight percent PCBM.

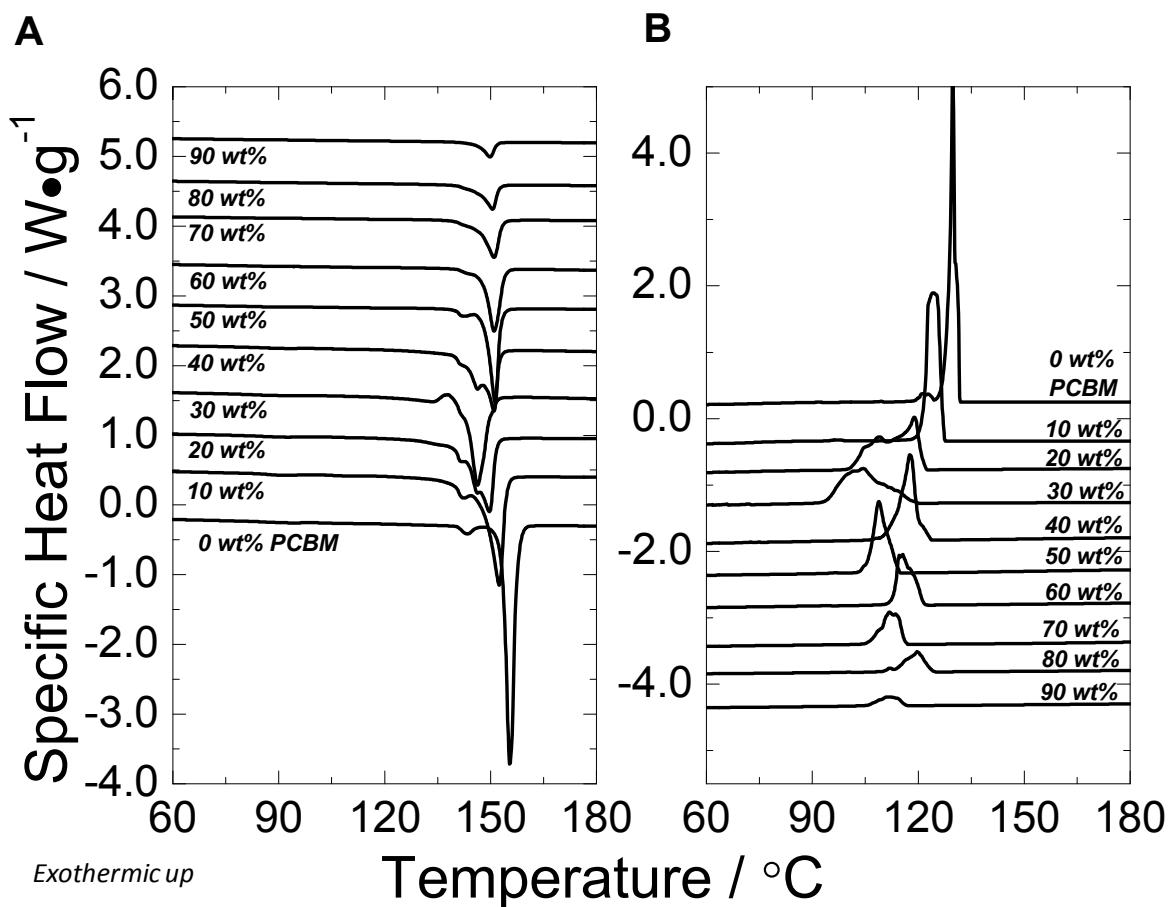


Figure S11. Differential scanning calorimetry thermograms of BD6:PCBM composition series mixtures dried from chlorobenzene for (A) 2nd heating cycle and (B) 2nd cooling cycle. Cycles are taken from -60 $^{\circ}\text{C}$ to 200 $^{\circ}\text{C}$. Thermograms have been truncated to show the thermal transitions better. Thermograms have been offset for better display. Each composition is demarcated by weight percent PCBM.

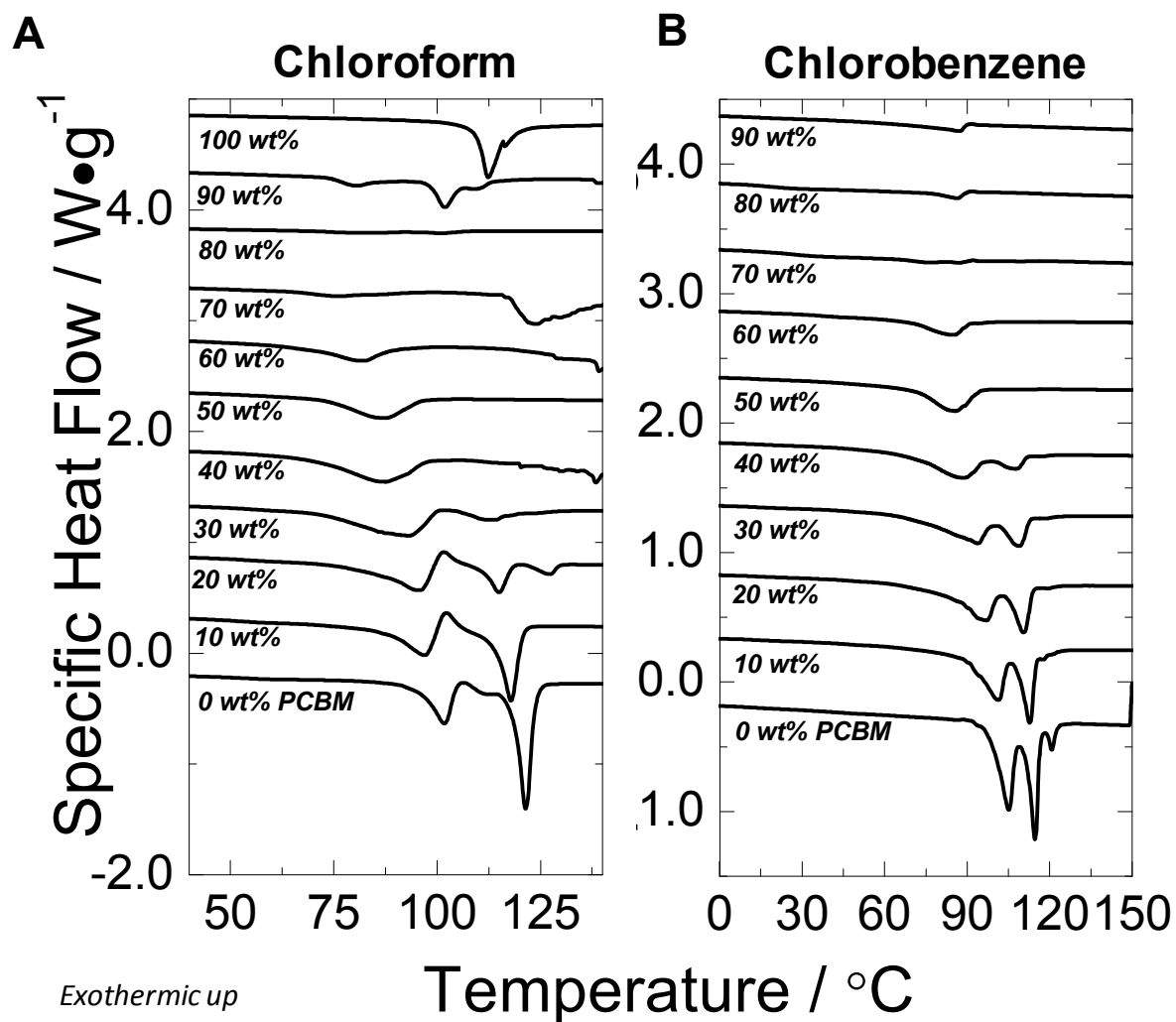


Figure S12. Differential scanning calorimetry thermograms of 1st heating cycle for BD:PCBM composition series mixtures dried from (A) chloroform and (B) chlorobenzene. Cycles are taken from -60 °C to 200 °C. Thermograms have been truncated to show the thermal transitions better. Thermograms have been offset for better display. Each composition is demarcated by weight percent PCBM.

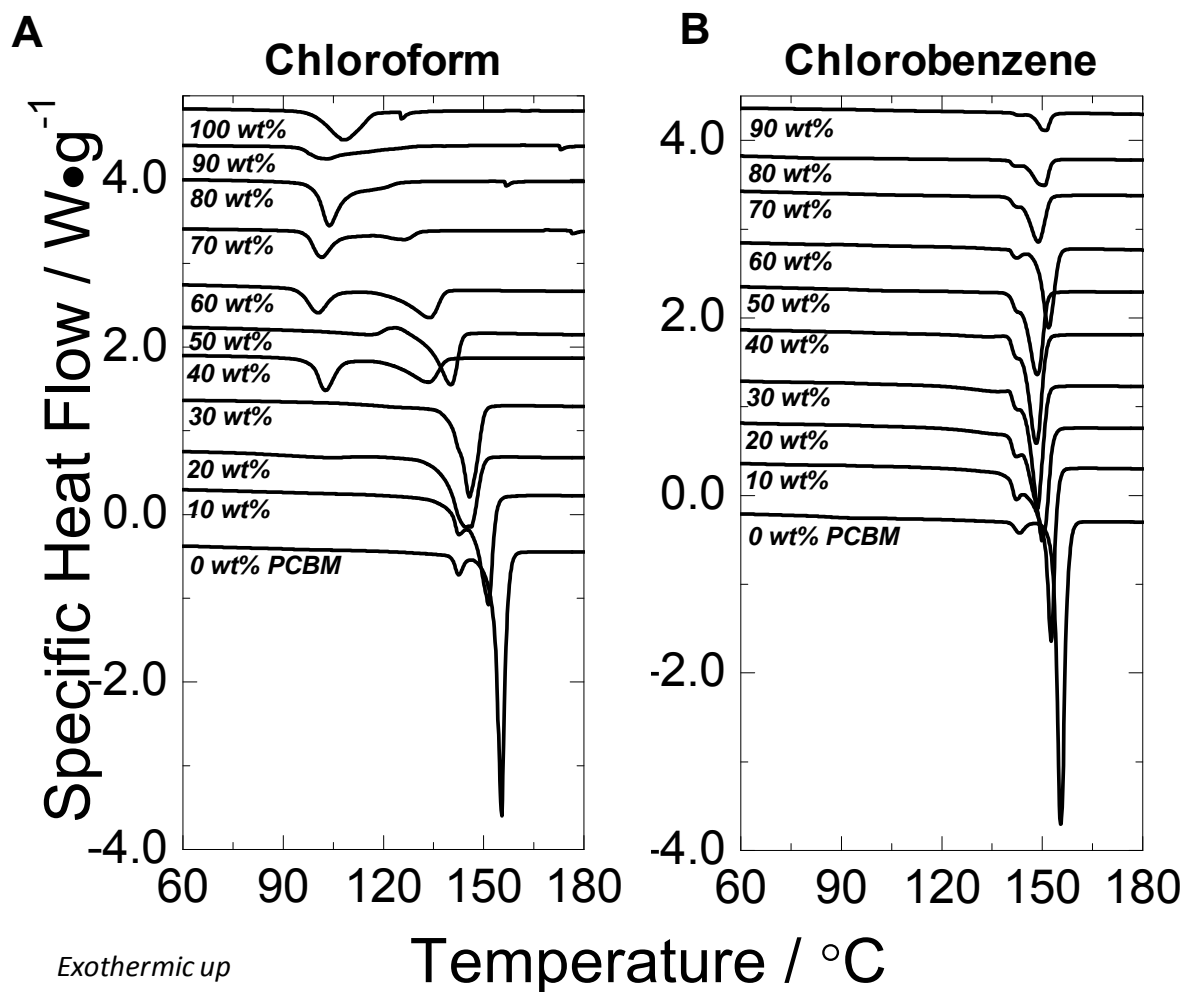


Figure S13. Differential scanning calorimetry thermograms of 1st heating cycle for BD6:PCBM composition series mixtures dried from (A) chloroform and (B) chlorobenzene. Cycles are taken from -60 °C to 200 °C. Thermograms have been truncated to show the thermal transitions better. Thermograms have been offset for better display. Each composition is demarcated by weight percent PCBM.

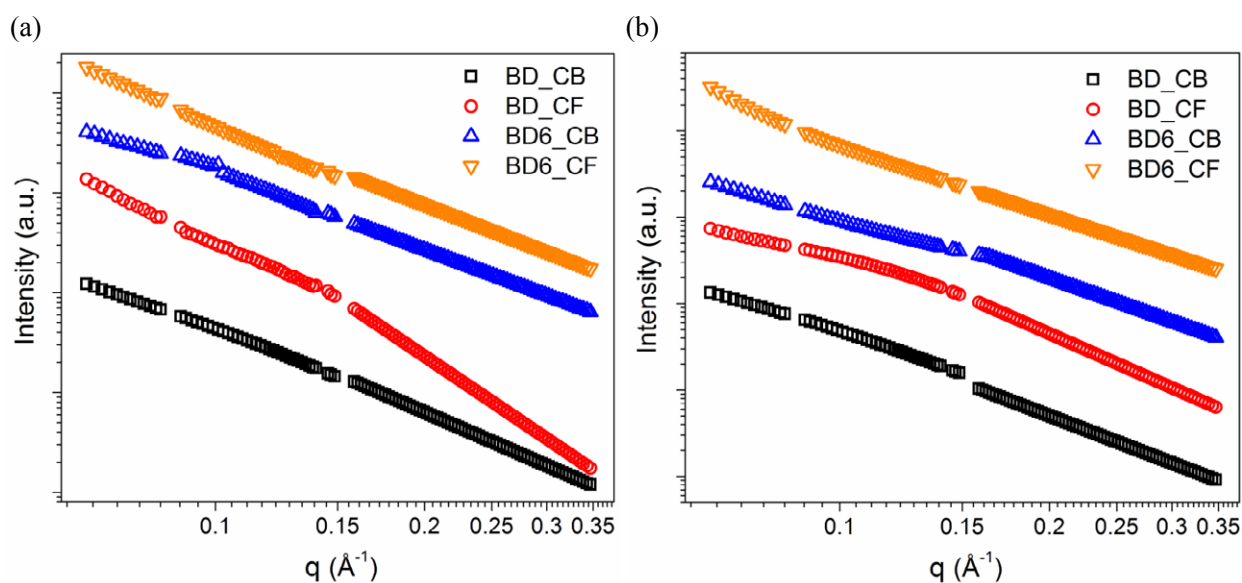


Figure S14. Integrated scattering intensity as a function of scattering vector from the raw two-dimensional scattering patterns for samples with (a) 1:1 donor-to-acceptor ratio and (b) 1:2 donor-to-acceptor ratio. CF denotes chloroform and CB denotes chlorobenzene as the solvent used in the sample preparation.

The scattering intensity as a function of the scattering vector presented in Figure S14 can be converted into Porod plots by plotting I/Q vs. q^{-4} , where I is the scattering intensity, q is the scattering vector, and Q is an invariant defined as:¹³

$$Q = \frac{1}{2\pi^2} \int_0^\infty q^2 \cdot I \cdot dq \quad (\text{S1})$$

The Porod plots are summarized in Figure S15.

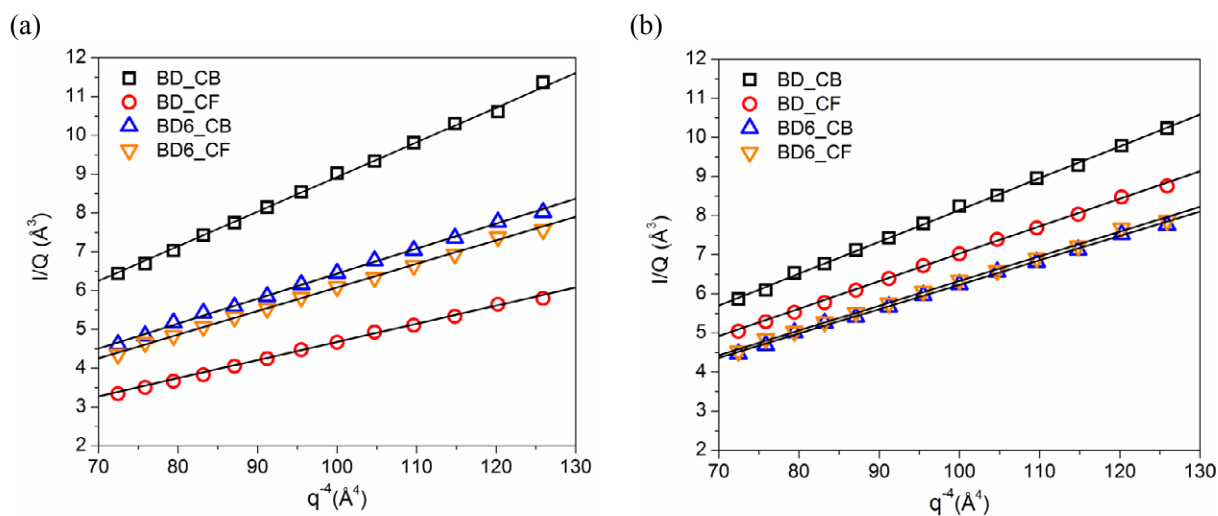


Figure S15. Porod plots for samples with (a) 1:1 donor-to-acceptor ratio and (b) 1:2 donor-to-acceptor ratio. The discrete symbols are the raw data, and the solid lines are the best fit using a linear equation with an intercept of zero. CF denotes chloroform and CB denotes chlorobenzene as the solvent.

The donor-acceptor interface surface area-to-volume ratio (S/V) can then be deduced using the Porod Law:¹³

$$\frac{I}{Q} = \frac{2\pi}{\phi_1\phi_2} \frac{S}{V} \frac{1}{q^4} \quad (\text{S2})$$

where ϕ_1 and ϕ_2 are the volume fractions of the donor and acceptor respectively. In this study, the values of the weight fractions were used to approximate the volume fractions. The deduced S/V values are given in Table S2.

Table S2. Interfacial Surface Area-to-Volume Ratios (S/V) Deduced from Porod Analysis

Donor	Donor-to-Acceptor Ratio	Solvent	S/V (10^{-3} \AA^{-1})
BD	1:1	Chlorobenzene	3.55
BD	1:1	Chloroform	1.86
BD6	1:1	Chlorobenzene	2.56
BD6	1:1	Chloroform	2.42
BD	1:2	Chlorobenzene	2.87
BD	1:2	Chloroform	2.48
BD6	1:2	Chlorobenzene	2.48
BD6	1:2	Chloroform	2.52

Table S3. Hildebrand (δ_T) and Hansen (δ_D = dispersion, δ_P = electrostatics, δ_H = hydrogen bonding) solubility parameters and density of the donor and acceptor molecules used in the study computed from molecular dynamics simulations.¹⁴ The unit for the solubility parameters is in $(\text{cal}/\text{cm}^3)^{0.5}$; densities are given in g/cm^3 .

	Simulations (300 K)				Experiment (298 K)			
	Density	δ_T	δ_D	$(\delta_P+\delta_H)$	Density	δ_T	δ_D	$(\delta_P+\delta_H)$
<i>amorphous</i>								
BD	1.27	10.23	10.17	1.18	-	-	-	-
BD6	1.16	9.76	9.50	2.24	-	-	-	-
PCBM ¹¹	1.52	10.65	9.87	3.99	1.51	10.69	9.97	3.86

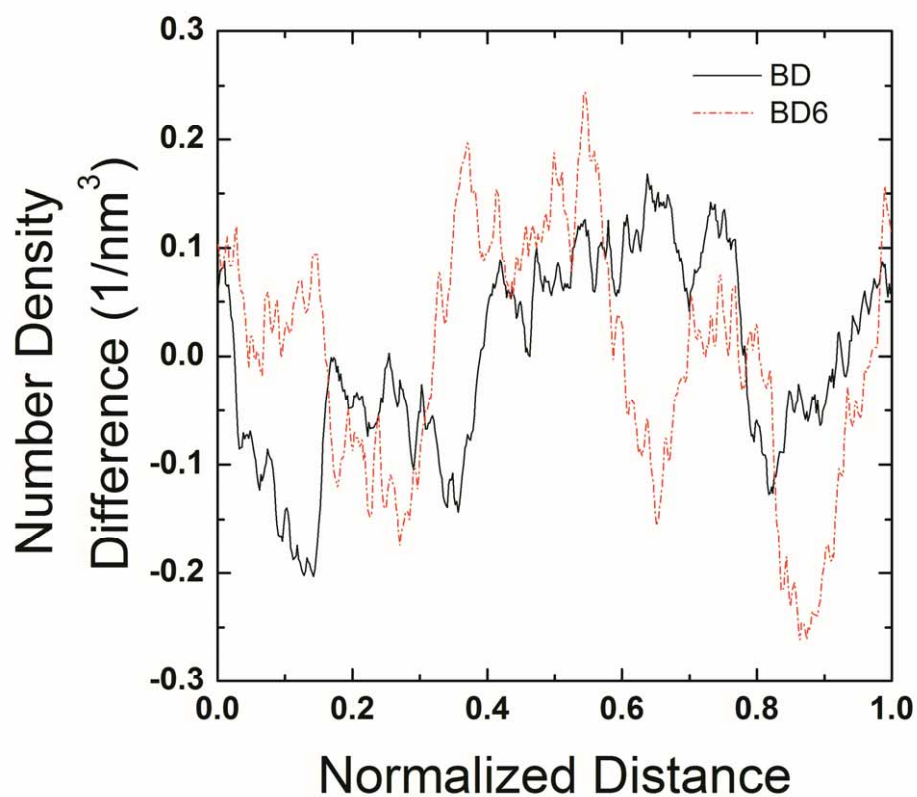


Figure S16. Density difference between donor and acceptor molecules in mixtures of 50 mol% PCBM. When the number of PCBM and BDX molecules are equal in the xy-plane of the simulation box the number density difference is zero; negative values indicate a PCBM rich phase and positive values indicate a BDX rich phase.

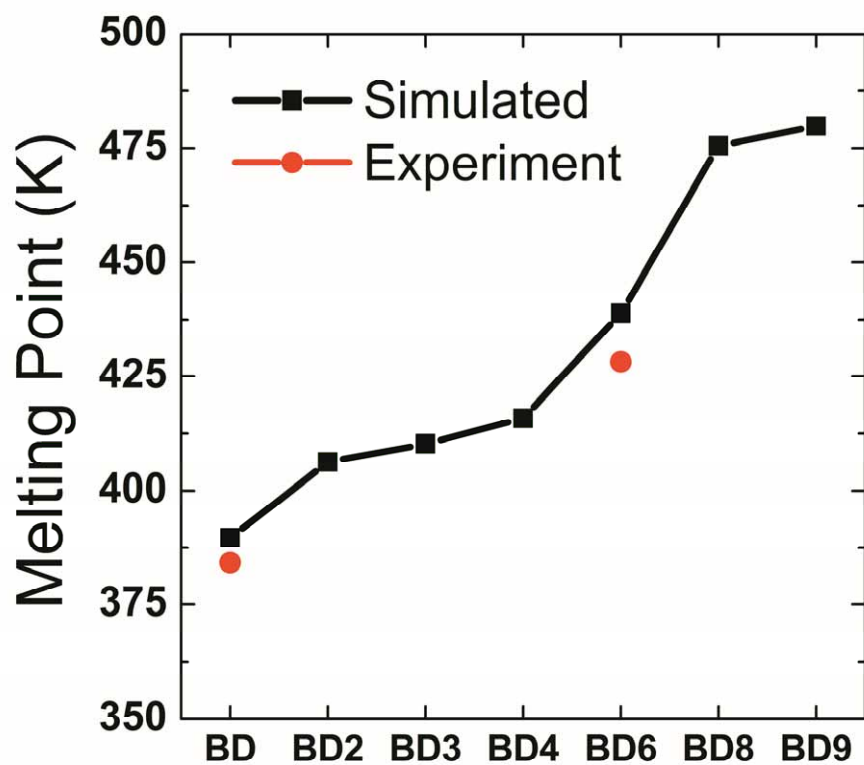


Figure S17. Simulated melting temperatures for different BDX molecules as a function of the length of the aliphatic side chain attached to the α -position of benzothiadiazole.

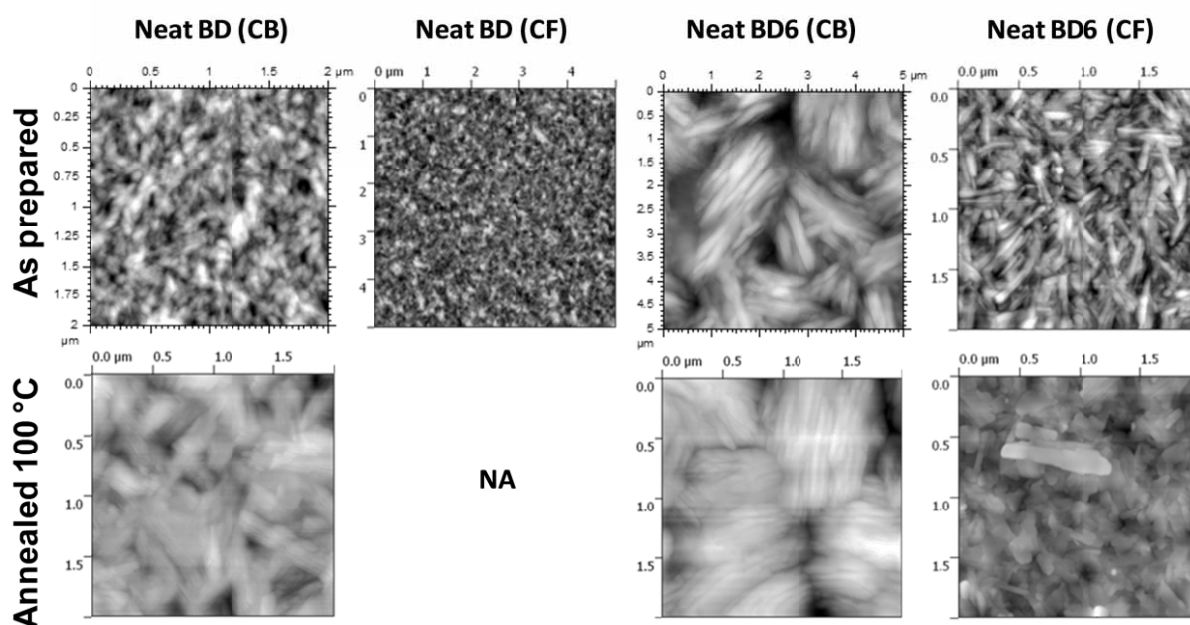


Figure S18. Atomic force microscopy topography scans of neat films of BD and BD6 prepared from chlorobenzene (CB) and chloroform (CF) in the as-prepared state and after annealing at 100 °C.

References

1. L. E. Polander, L. Pandey, S. Barlow, S. P. Tiwari, C. Risko, B. Kippelen, J.-L. Bredas and S. R. Marder, *J. Phys. Chem. C*, 2011, **115**, 23149-23163.
2. Free software available from <http://gwyddion.net/>.
3. W. L. Jorgensen, E. R. Laird, T. B. Nguyen and J. Tirado-Rives, *J. Comput. Chem.*, 1993, **14**, 206-215.
4. W. L. Jorgensen, D. S. Maxwell and J. Tirado-Rives, *J. Am. Chem. Soc.*, 1996, **118**, 11225-11236.
5. H. J. C. Berendsen, D. Vandespoel and R. Vandrunen, *Comput. Phys. Commun.*, 1995, **91**, 43-56.
6. B. Hess, C. Kutzner, D. van der Spoel and E. Lindahl, *J. Chem. Theory Comput.*, 2008, **4**, 435-447.
7. S. W. Watt, J. A. Chisholm, W. Jones and S. Motherwell, *J. Chem. Phys.*, 2004, **121**, 9565-9573.
8. J. H. Hildebrand and R. L. Scott, *J. Chem. Phys.*, 1952, **20**, 1520-1521.
9. C. M. Hansen, *J Paint Techn.*, 1967, **39**, 104.
10. M. Belmares, M. Blanco, W. A. Goddard, R. B. Ross, G. Caldwell, S. H. Chou, J. Pham, P. M. Olofson and C. Thomas, *J. Comput. Chem.*, 2004, **25**, 1814-1826.
11. N. R. Tummala, Y. T. Fu, S. Mehraeen, C. Risko and J.-L. Brédas, *Adv. Funct. Mater.*, 2013, DOI:10.1002/adfm.201300918.
12. A. P. Hammersley, S. O. Svensson, M. Hanfland, A. N. Fitch and D. Hausermann, *High Pressure Res.*, 1996, **14**, 235-248.
13. R. J. Roe, *Methods of X-ray and neutron scattering in polymer science*, New York, Oxford University Press, 2000.
14. From the MD simulations, determination of the hydrogen bond energy is not straightforward and would require separating the Coulombic interactions into dipole-dipole and hydrogen bond interactions through specification of an arbitrary cut-off. We therefore only report Hildebrand parameters and the contributions from the dispersive and Coulombic interactions. Since Hildebrand solubility parameters are for pure components, we do not report parameters for the donor-acceptor mixtures.